Hot Spots Conjecture and Its Application to Modeling Tubular Structures

Moo K. Chung[1,2,3,4], Seongho Seo[4], Nagesh Adluru[2], and Houri K. Vorperian[3]

[1] Department of Biostatistics and Medical Informatics
[2] Waisman Laboratory for Brain Imaging and Behavior
[3] Vocal Tract Development Laboratory, Waisman Center
University of Wisconsin, Madison, WI 53706, USA
[4] Department of Brain and Cognitive Sciences
Seoul National University, Korea
mkchung@wisc.edu

Abstract. The second eigenfunction of the Laplace-Beltrami operator follows the pattern of the overall shape of an object. This geometric property is well known and used for various applications including mesh processing, feature extraction, manifold learning, data embedding and the minimum linear arrangement problem. Surprisingly, this geometric property has not been mathematically formulated yet. This problem is directly related to the somewhat obscure *hot spots conjecture* in differential geometry. The aim of the paper is to raise the awareness of this nontrivial issue and formulate the problem more concretely. As an application, we show how the second eigenfunction alone can be used for complex shape modeling of tubular structures such as the human mandible.

1 Introduction

The second eigenfunction of the Laplace-Beltrami operator is drawing significant attention in recent years mainly as a tool for extracting shape features in high dimensional data [2,8,10]. The gradient of eigenfunction tends to follow the pattern of the overall shape of data and has been used to establish the intrinsic coordinate system of the data. This geometric property has been well known and often been used in computer vision and medical imaging applications. The second eigenfunction of the graph Laplacian was used to construct the Laplacian eigenmaps for low dimensional embedding [2]. The critical points of the second eigenfunction were used as anatomical landmarks for piecewise registration of colon surfaces [8]. The Reeb graph of the second eigenfunction was used in characterizing hippocampus shape [10].

All these studies rely on the geometric property of the second eigenfunction and somehow captures the overall shape of data. However, this property has not been mathematically formulated precisely. In fact, it is related to an obscure conjecture called the hot spots conjecture in differential geometry [1]. In this
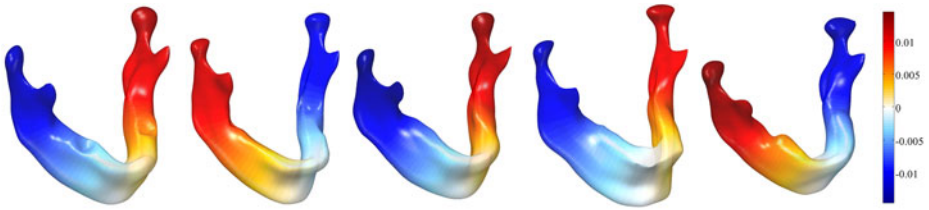
Fig. 1. The second eigenfunction ψ_1 for different mandible surfaces. The second eigenfunction for an elongated closed object is a smooth monotonic function increasing from one tip of surface to the other tip of the surface.

paper, we will explore the issue in detail and formulate the geometric property more precisely, which will be illustrated with examples and a proof for simple shape.

2   The Second Laplace-Beltrami Eigenfunction

Second Eigenfunction. The eigenfunctions of the Laplace-Beltrami operator has been used in many different contexts in image analysis [8,9,10]. Eigenfunctions ψ_j of Laplace-Beltrami operator Δ in $\mathcal{M}$ satisfy $\Delta\psi_j = \lambda_j\psi_j$. The eigenfunctions form an orthonormal basis in $\mathcal{M}$. We can order the eigenfunctions $\psi_0, \psi_1, \psi_2, \cdots$ corresponding to the increasing order of eigenvalues $0 = \lambda_0 \leq \lambda_1 \leq \lambda_2 \leq \cdots$. Other than $\psi_0 = 1/\sqrt{\mu(M)}$, the close form expression for other eigenfunctions are unknown. However, using the cotan discretization for the Laplace-Beltrami operator [3,9], we can obtain the eigenfunctions numerically. The MATLAB code is available at `http://brainimaging.waisman.wisc.edu/~chung/lb`.

The critical point of the second eigenfunction ψ_1 usually occur at the two extremes of an elongated object (Figure 1). So the gradient of the second eigenfunction follows the shape of elongated objects. In computer vision literature, this *monotonicity property* was observed but without any mathematical justification [2,10]. Many treated it as a proven fact although the underlying conjecture has yet to be proved [1].

Conjecture 1. (Rauch's hot spots conjecture) [1] Let $\mathcal{M}$ be an open connected bounded subset. Let $f(\sigma, p)$ be the solution of heat equation

$$\frac{\partial f}{\partial \sigma} = \Delta f \tag{1}$$

with the initial condition $f(0, p) = g(p)$ and the Neumann boundary condition $\frac{\partial f}{\partial n}(\sigma, p) = 0$ on the boundary $\partial\mathcal{M}$. Then for *most* initial conditions, if p_{hot} is a point at which the function $f(\cdot, p)$ attains its maximum (hot spot), then the distance from p_{hot} to $\partial\mathcal{M}$ tends to zero as $\sigma \to \infty$ [1].

We can also claim a similar statement for minimum (cold spots) as well. Conjecture 1 basically implies that the hot and cold spots move away from the
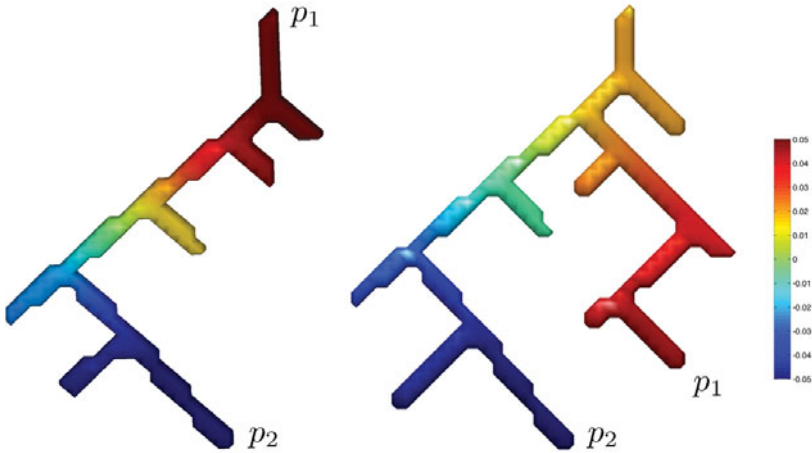
Fig. 2. The second eigenfunction ψ_1 of branching tubular structures. The maximum (p_1) and the minimum (p_2) of ψ_1 always occur at the points of maximum geodesic distance.

origin toward the boundary as the diffusion continues. Note that the solution to heat equation (1) is given by heat kernel expansion [9]:

$$K_\sigma * g(p) = \sum_{j=0}^{\infty} e^{-\lambda_j \sigma} \beta_j \psi_j(p), \tag{2}$$

where $\beta_j = \langle \psi_j, g \rangle$ are Fourier coefficients. Since $\lambda_0 = 0$ and $\psi_0 = 1/\sqrt{\mu(\mathcal{M})}$, we have

$$K_\sigma * g(p) = \frac{\int_{\mathcal{M}} g(p) \, d\mu(p)}{\mu(\mathcal{M})} + \beta_1 e^{-\lambda_1 \sigma} \psi_1(p) + R(\sigma, p), \tag{3}$$

where the first term is the average signal and the remainder R goes to zero faster than $e^{-\lambda_1 \sigma}$ as $\sigma \to \infty$ [1] . Therefore, the behavior of the propagation of the hot spots is basically governed by the eigenfunction ψ_1.

What will happen if there is no boundary? In the case of closed manifold with no boundary, the Neumann boundary condition simply disappears so the direct application of the hot spots conjecture is not valid. Since ψ_1 asymptotically behaves like the heat equilibrium state, hot and cold spots cannot possibly be located in close proximity. Thus, we propose the following conjecture.

Conjecture 2. For a closed and sufficiently smooth simply connected surface $\mathcal{M}$ with no boundary, the geodesic distance d between any two points p and q is bounded by

$$d(p, q) \leq d(p_{min}, p_{max}).$$

Conjecture 2 implies that the hot and cold spots give the maximum possible geodesic distance among all possible pairs of points and define the direction

of elongation of data. Figure 2 illustrates Conjecture 2. For any complicated branching binary tree structures like Figure 2, the hot and cold spots occur at the two extreme points along the longest geodesic path. The hot spots conjecture basically dictates that it is possible to find the maximum possible geodesic path by simply finding the critical points in the second eigenfunction. Conjecture 2 can be applicable not only to differentiable manifolds but to graphs and surface meshes as well.

3   Hot Spots Conjecture Applied to Fiedler's Vector

Surface meshes can be considered as graphs. The connection between the eigenfunctions of continuous and discrete Laplacians has been well established by many authors [6,11]. Many properties of eigenfunctions of the Laplace-Beltrami operator have discrete analogues. The second eigenfunction of the discrete graph Laplacian is called the Fiedler vector and it has been studied in connection to the graph and mesh processing, manifold learning and the minimum linear arrangement problem [5] Let $G = \{V, E\}$ be the graph with the vertex set V and the edge set E. G is the discrete approximation of the underlying continuous manifold $\mathcal{M}$. We will simply index the node set as $V = \{1, 2, \cdots, n\}$. If two nodes i and j form an edge, we denote it as $i \sim j$. Various forms of graph Laplacian have been proposed but many graph or discrete Laplacian $L = (l_{ij})$ is a real symmetric matrix of the form

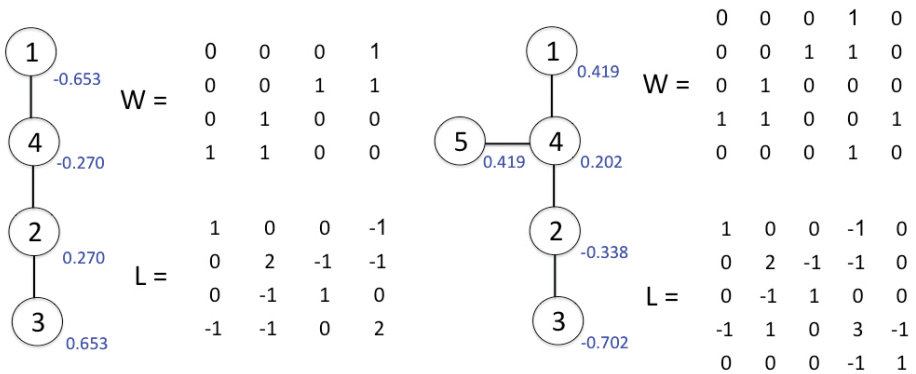$$l_{ij} = \begin{pmatrix} -w_{ij}, & i \sim j \\ \sum_{i \neq j} w_{ij}, & i = j \\ 0, & \text{otherwise} \end{pmatrix}$$

$$W = \begin{pmatrix} 0 & 0 & 0 & 1 \\ 0 & 0 & 1 & 1 \\ 0 & 1 & 0 & 0 \\ 1 & 1 & 0 & 0 \end{pmatrix} \qquad W = \begin{pmatrix} 0 & 0 & 0 & 1 & 0 \\ 0 & 0 & 1 & 1 & 0 \\ 0 & 1 & 0 & 0 & 0 \\ 1 & 1 & 0 & 0 & 1 \\ 0 & 0 & 0 & 1 & 0 \end{pmatrix}$$

$$L = \begin{pmatrix} 1 & 0 & 0 & -1 \\ 0 & 2 & -1 & -1 \\ 0 & -1 & 1 & 0 \\ -1 & -1 & 0 & 2 \end{pmatrix} \qquad L = \begin{pmatrix} 1 & 0 & 0 & -1 & 0 \\ 0 & 2 & -1 & -1 & 0 \\ 0 & -1 & 1 & 0 & 0 \\ -1 & 1 & 0 & 3 & -1 \\ 0 & 0 & 0 & -1 & 1 \end{pmatrix}$$

Node values (a): 1: -0.653, 4: -0.270, 2: 0.270, 3: 0.653

Node values (b): 1: 0.419, 5-4 edge: 0.419, 4: 0.202, 2: -0.338, 3: -0.702

Fig. 3. A graph, the weights W and the graph Laplacian L. The weights are simply the adjacency matrix. The second eigenfunction ψ_1 value is displayed in blue. (a) This example is given in [7]. The maximum geodesic distance is obtained between the nodes 1 and 3, which are also hot and cold spots. (b) In this example, there are two hot spots 1 and 5 which correspond to two maximal geodesic paths 1-4-2-3 and 5-4-2-3.

for some edge weight w_{ij}. The graph Laplacian L can be decomposed as $L = D - W$, where $D = (d_{ij})$ is the diagonal matrix with $d_{ii} = \sum_{j=1}^{n} w_{ij}$ and $W = (w_{ij})$. For a vector $\mathbf{f} = (f_1, \cdots, f_n)'$ observed at the n nodes, the discrete analogue of the Dirichlet energy is given by

$$\mathcal{E}(f) = \mathbf{f}' L \mathbf{f} = \sum_{i,j=1}^{n} w_{ij}(f_i - f_j)^2 = \sum_{i \sim j} w_{ij}(f_i - f_j)^2. \tag{4}$$

The Fiedler's vector $\boldsymbol{f} = (f_1, \cdots, f_n)'$ is obtained as the minimizer of the quadratic polynomial $\psi_1 = \arg\min_{\boldsymbol{f}} \mathcal{E}(\mathbf{f})$ subject to the quadratic constraint $\|\mathbf{f}\|^2 = \sum_i f_i^2 = 1$. The Dirichlet energy measures the smoothness of $\mathbf{f}$ so the second eigenfunction should be the smoothest possible map among all possible functions. Since ψ_1 is required to be orthonormal with ψ_0, we also have an additional constraint $\sum_i f_i = 0$. Therefore, ψ_1 is positive on half of $\mathcal{M}$ and negative on the other half. However, it still does not explicitly tell us that a smooth function has to be monotonically changing from one end to the other.

The constraints force ψ_1 to have at least two differing *sign domains* in which ψ_1 has one sign. The *nodal set* of eigenfunctions ψ_i is defined as the zero level set $\psi_i(p) = 0$. Then Courant's nodal line theorem states that the nodal set of the i-th eigenfunction ψ_{i-1} divide the manifold into no more than i sign domains [4,6,11]. Hence, the second eigenfunction must have exactly 2 disjoint sign domains. At the positive sign domain, we have the global maximum and at the negative sign domain, we have the global minimum. This is illustrated in Figure 3 and 4. Although it is difficult to prove the general statement, the conjecture can be proven for specific cases. Here we provide a first heuristic proof for a path, which is a graph with maximal degree 2 and without a cycle.

Tightness. For a function $\mathbf{f}$ defined on the vertex set V, let G_s^- be the subgraph induced by the vertex set $V_s^- = \{i \in V | f_i < s\}$. Similarly, let G_s^+ be the subgraph induced by the vertex set $V_s^+ = \{i \in V | f_i > s\}$. For any s, if G_s^- and G_s^+ are either connected or empty, then $\mathbf{f}$ is tight [11]. The concept of tightness is crucial in proving the statement. When $s = 0$, G_0^+ and G_0^- are sign graphs. If we relax the condition so that G_s^+ contains nodes satisfying $f_i \geq s$, we have *weak sign graphs*. The second eigenfunction on a graph with maximal degree 2 (either cycle or path) is tight [11]. Figure 4 shows an example of a path with 11 nodes. Among three candidates for the second eigenfunction, (a) and (b) are not tight while (c) is. Note that the candidate function (a) has two disjoint components when thresholded at $s = 0.5$ so it cannot be tight. In order to be tight, the second eigenfunction cannot have a positive minimum or a negative maximum at the interior vertex in the graph [6]. This implies that the second eigenfunction must decrease monotonically from the positive to negative sign domains as shown in (c) and have the critical points at the two end points. This has to be true for a general case as well.
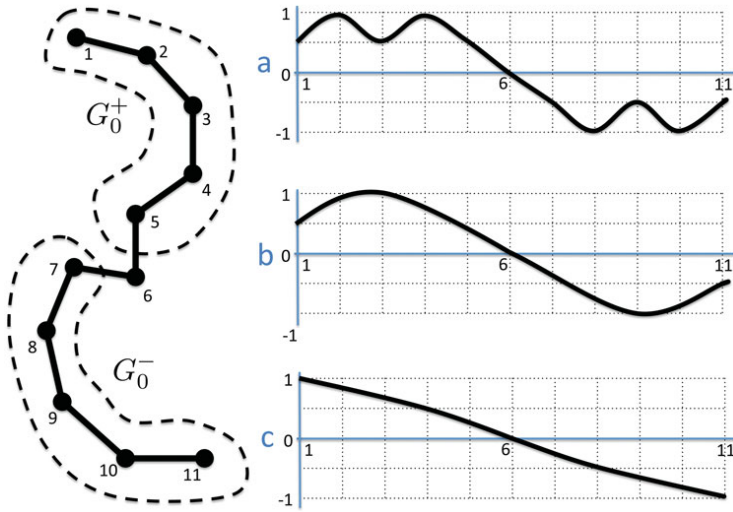
Fig. 4. A path with positive (G_0^+) and negative (G_0^-) sign domains. Among many possible candidate functions, (a) and (b) are not tight so they can't be the second eigenfunctions.
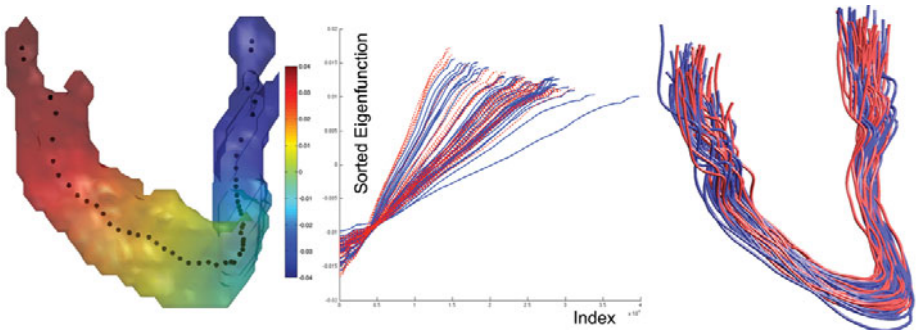

Fig. 5. Left: The centroids of level contours of the 2nd eigenfunction. Middle: The sorted second eigenfunctions (female =red, male = blue). Right: The centerlines of all 76 subjects showing the proper alignment.

4 Application: Mandible Growth Modeling

The CT imaging data set consists of 76 mandibles (40 males and 36 females). The age distribution was 11.33 ± 5.60 years for the females, and 9.54 ± 5.71 years for the males. The image acquisition and processing details for acquiring the mandible surface meshes are given in [9].

Features. In most literature dealing with the eigenfunctions of the Laplace-Beltrami operator, the whole spectrum of eigenvalues or eigenfunctions were used for shape analysis [9,10]. Here, we show how the second eigenfunction alone can be used as the shape feature. Once we obtained the second eigenfunctions for all subjects, we sorted them in increasing order (Figure 5). The sorted eigenfunctions are almost straight lines. A bigger mandible (more indices) exhibits a less steeper slope. Therefore, the rate of increase of the sorted eigenfunction (slope of linear fit) can be used for characterizing subject anatomical variability.

General Linear Models. We examined how the rate of increase can be used in characterizing the growth of the mandible. We used the general linear model (GLM) of the form `feature` $= \beta_0 + \beta_1$ `gender` $+ \beta_2$ `age` $+ \epsilon$. The parameters are estimated using the least squares method and the statistical significance is determined using the F-statistic. There is weakly significant gender difference (β_1) (p-value $= 0.08$) and highly significant age effect (β_2) (p-value $< 10^{-7}$) for the rate of increase. We conclude that the mandible size grows at a much faster rate for males than females.

References

1. Banuelos, R., Burdzy, K.: On the Hot Spots Conjecture of J Rauch. Journal of Functional Analysis 164, 1–33 (1999)
2. Belkin, M., Niyogi, P.: Laplacian eigenmaps and spectral techniques for embedding and clustering. In: Advances in Neural Information Processing Systems, vol. 1, pp. 585–592 (2002)
3. Chung, M.K., Taylor, J.: Diffusion smoothing on brain surface via finite element method. In: Proceedings of IEEE International Symposium on Biomedical Imaging (ISBI), vol. 1, pp. 432–435 (2004)
4. Courant, R., Hilbert, D.: Methods of Mathematical Physics, english edn. Interscience, New York (1953)
5. Fiedler, M.: Algebraic connectivity of graphs. Czechoslovak Mathematical Journal 23, 298–305 (1973)
6. Gladwell, G.M.L., Zhu, H.: Courant's nodal line theorem and its discrete counterparts. The Quarterly Journal of Mechanics and Applied Mathematics 55, 1–15 (2002)
7. Hall, K.M.: An r-dimensional quadratic placement algorithm. Management Science 17, 219–229 (1970)
8. Lai, Z., Hu, J., Liu, C., Taimouri, V., Pai, D., Zhu, J., Xu, J., Hua, J.: Intrapatient supine-prone colon registration in CT colonography using shape spectrum. In: Jiang, T., Navab, N., Pluim, J.P.W., Viergever, M.A. (eds.) MICCAI 2010. LNCS, vol. 6361, pp. 332–339. Springer, Heidelberg (2010)

9. Seo, S., Chung, M.K., Vorperian, H.K.: Heat kernel smoothing using laplace-beltrami eigenfunctions. In: Jiang, T., Navab, N., Pluim, J.P.W., Viergever, M.A. (eds.) MICCAI 2010. LNCS, vol. 6363, pp. 505–512. Springer, Heidelberg (2010)
10. Shi, Y., Lai, R., Krishna, S., Sicotte, N., Dinov, I., Toga, A.W.: Anisotropic Laplace-Beltrami eigenmaps: Bridging Reeb graphs and skeletons. In: Proceedings of Mathematical Methods in Biomedical Image Analysis (MMBIA), pp. 1–7 (2008)
11. Tlusty, T.: A relation between the multiplicity of the second eigenvalue of a graph laplacian, courants nodal line theorem and the substantial dimension of tight polyhedral surfaces. Electrnoic Journal of Linear Algebra 16, 315–324 (2007)